# Boundary Conditions Used in NIMROD Helicity Injection Simulations

C. R. Sovinec,[1] E. B. Hooper,[2] and J. B. O'Bryan[1]
[1]*University of Wisconsin-Madison*
[2]*Lawrence-Livermore National Laboratory*

Informal Discussion with NSTX-CHI Group
May 17, 2012

Some slides are from ICC 2011 and Sherwood 2012.
Also see Phys. Plasmas **18**, 094502.

**Introduction:** HIT and HIT-II were spherical torus (ST) experiments at U. WA designed to study coaxial helicity injection (CHI) current-drive.

- Unlike CHI in spheromaks, configurations with a conducting center column need an insulating absorber gap to allow steady-state operation, d(tor. flux)/dt $\rightarrow 0$.

- At large $I_{INJ}/I_{TF}$ ratios, MHD instabilities are excited, and the current-density profile relaxes.

**Domain for HIT-II computations**

- At smaller $I_{INJ}/I_{TF}$ ratios, explored in the 24954-24971 and 26449-26476 series, for example, any relaxation is relatively weak. HIT-II results in these conditions show distinct scaling information.

- Our present HIT-II modeling focuses on these weakly relaxing cases.

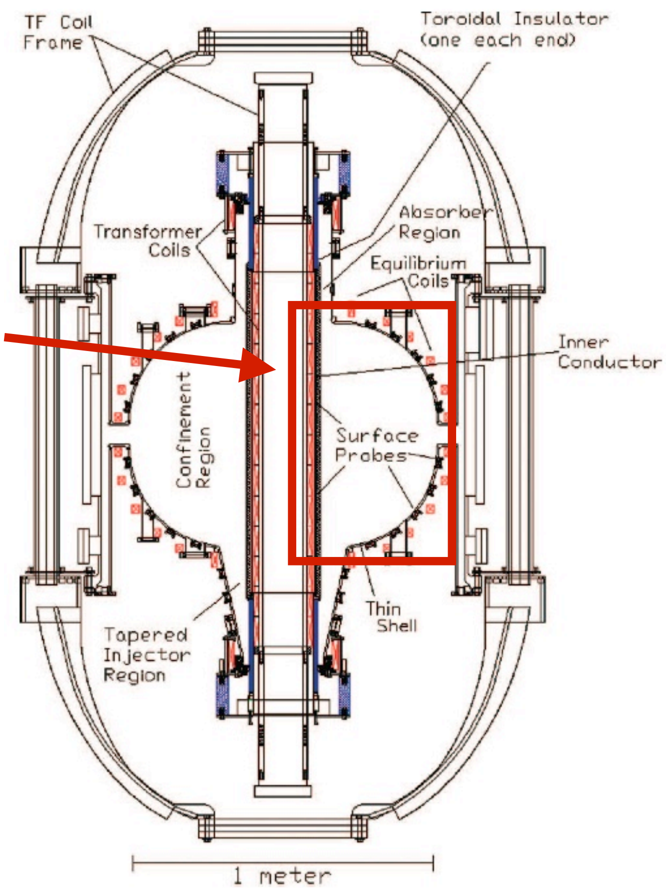


**Schematic of HIT-II cross section shows flux conserver shape, injector (bottom), and absorber (top).**

# All computations start from vacuum magnetic field.

• The initial poloidal flux distribution is computed from a set of external coils.

• The initial $I = RB_\phi$ is uniform, and its value is the prescribed $I_{TF}$.

• All simulated CHI dynamics are controlled by the absorber and injector boundary conditions and are outputs of the computations.

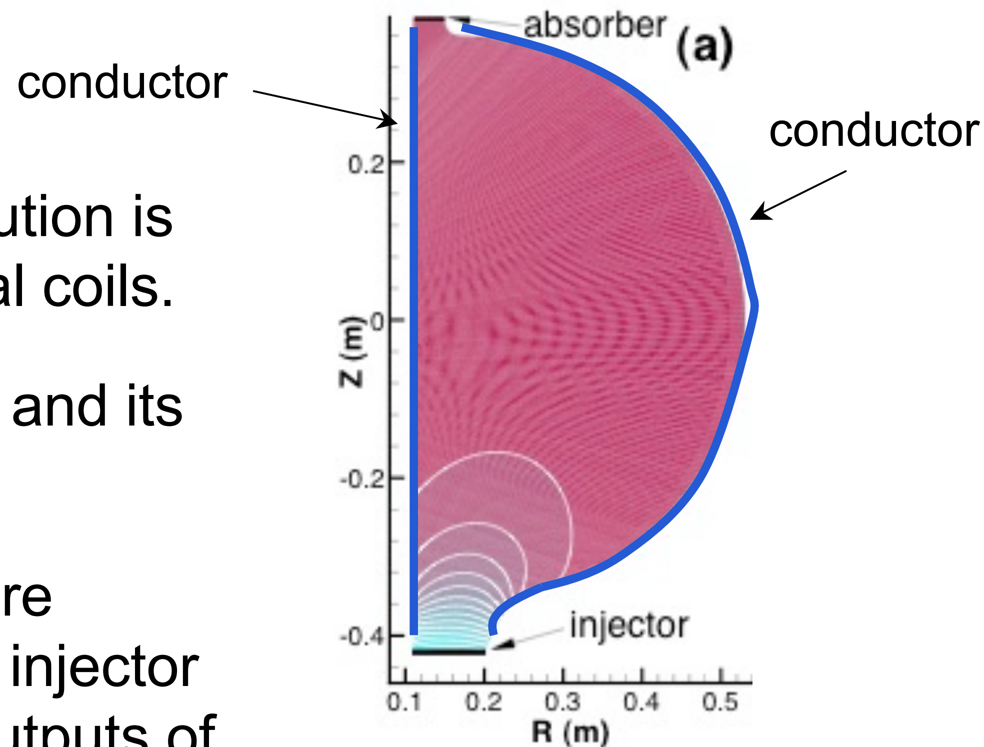


**This cross-section shows the initial poloidal flux distribution, and the geometry of the domain as represented by a 30×70 conforming mesh.**

# Basics: injecting current means that $I_{inj} \neq I_{abs}$.

- Conducting boundary conditions along the inboard and outboard surfaces do not admit or release toroidal flux.
- Boundary conditions along the injector and absorber allow local flux of $B_\phi$.
- $\Delta I = I_{inj}$ is small relative to $I_{TF}$ in tokamak cases.
- The objective of the HIT-II study was steady-state behavior at varied $I_{TF}$ and $\psi_{inj}$.
    - In steady state, $V_{inj} = V_{abs}$.
        - Resistivity affects how much $I_{inj}$ is produced at a given voltage.
        - Force-balance and $\psi_{inj}$ determine the distribution of **J**.
    - Raised $I_{inj}$ vs. lowered $I_{abs}$ (relative to prescribed $I_{TF}$) is inconsequential.

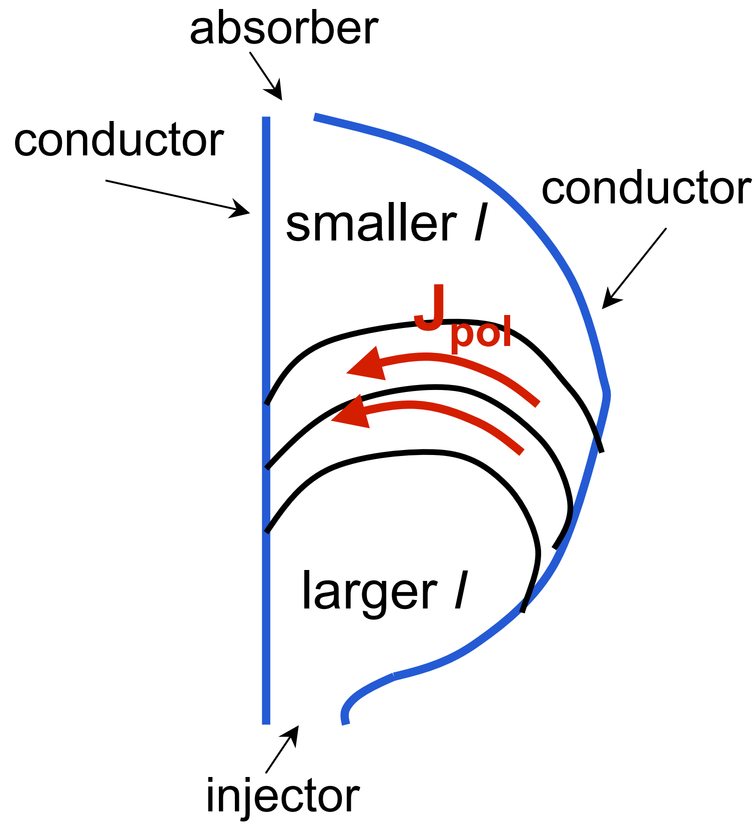


**Illustration of contours of constant $I=RB_\phi$ during injection.**

## **HIT-II Modeling & BCs:** At low-$\beta$, pressure has little influence on the 2D profiles, allowing simplified modeling.

- We model these discharges with the zero-$\beta$ limit of resistive MHD.

$$\rho\left(\frac{\partial}{\partial t}\mathbf{V}+\mathbf{V}\cdot\nabla\mathbf{V}\right)=\mathbf{J}\times\mathbf{B}+\nabla\cdot\left[\rho\nu\left(\nabla\mathbf{V}+\nabla\mathbf{V}^{T}-\frac{2}{3}\mathbf{I}\nabla\cdot\mathbf{V}\right)\right]$$
$$\frac{\partial}{\partial t}\mathbf{B}=\nabla\times\left(\mathbf{V}\times\mathbf{B}-\eta\mathbf{J}\right)$$

  - Mass density $\rho$ is considered a uniform constant.

- With viscosity, tangential-**V** (flow) is set to 0 along all boundaries.
- The normal component of **V** is zero along the conductors and nonzero along the injector and absorber.
- In NIMROD, equations are solved in weak form. For all test vectors **A**, determine **B** such that

$$\int\mathbf{A}\cdot\frac{\partial}{\partial t}\mathbf{B}\,dVol=\int\left(\mathbf{V}\times\mathbf{B}-\eta\mathbf{J}\right)\cdot\nabla\times\mathbf{A}\,dVol+\oint\mathbf{A}\cdot\mathbf{E}\times d\mathbf{S}$$

  - The mathematics allows specification of either tangential-**B** or -**E** along boundaries.

# The NIMROD boundary conditions need to represent both the injector gap and the absorber gap.

• Voltage in the HIT-II experiment is applied across the injector, and physics determines the voltage along other paths.

• With NIMROD, we may either specify a tangential electric field (Neumann condition) along a gap or $B_\phi$ (Dirichlet condition).

• $E_t = 0$ along the conductors.

• Applying $E_t \neq 0$ along both gaps presumes knowledge of the rate-of-change of flux as a function of time--not appropriate/practical.

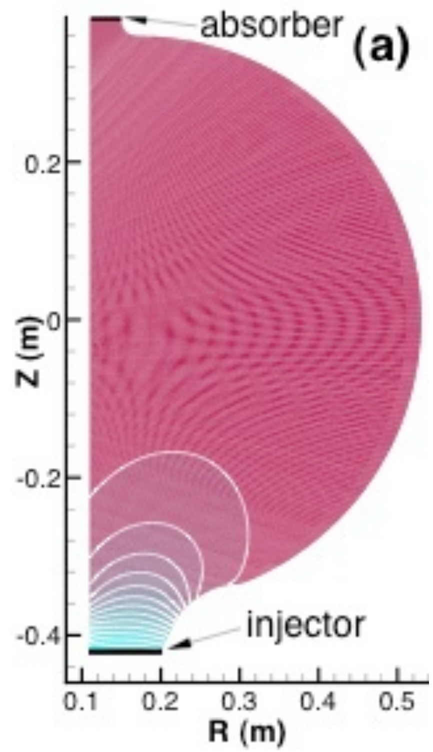


**This cross-section shows the initial poloidal flux distribution, and the geometry of the domain as represented by a 30×70 conforming mesh.**

# Applying a combination of the two possible magnetic-field boundary conditions is effective.

- For HIT-II modeling, we choose to apply $E_t$ along the absorber and $RB_\phi$, i.e. $\Delta I$ -value, along the injector.
    - Resistive MHD determines **E** everywhere below the absorber.
    - Outflow at the absorber is set to the **n·E×B**/$B^2$ drift speed to avoid a resistive boundary layer (~surface current).
    - Inflow at the injector is set to preserve plasma volume, i.e. avoid compression.
- If there is a mismatch in these specifications, $B_\phi$ along the absorber changes from its initial vacuum value. This represents current beyond the absorber gap, and we subtract this to obtain net injected current, $I_{INJ}$.
    - Experimental absorber arcs are analogous.

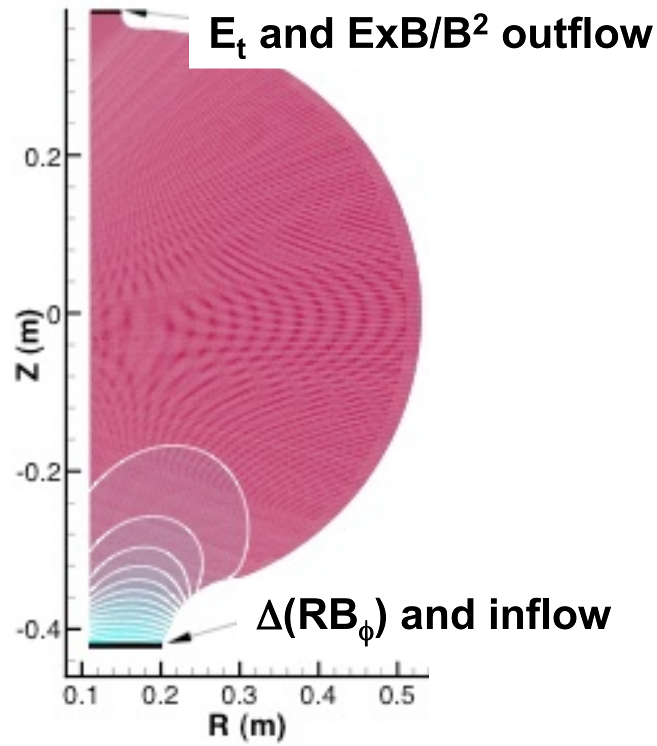


**Boundary conditions specified at the two gaps are indicated.**

# NIMROD results: An example result shows the expanded flux distribution after applying voltage at the absorber and current at the injector.

- In the case presented at right, we set $V$=37 V at the absorber, and $\Delta I$ at the injector for 30 kA.
    - $I_{TF}$ drifts from 495 kA to 516 kA.
    - Net $I_{INJ}$ is 8.8 kA.
    - Final $I_p$=91 kA (>10×$I_{INJ}$).
- The final current density profile is a hollow toroidal layer.
- The voltage is well below the experimental values of 600-700 V. Resistivity in the computations is based on the peak observed $T_e$, and there is no sheath.

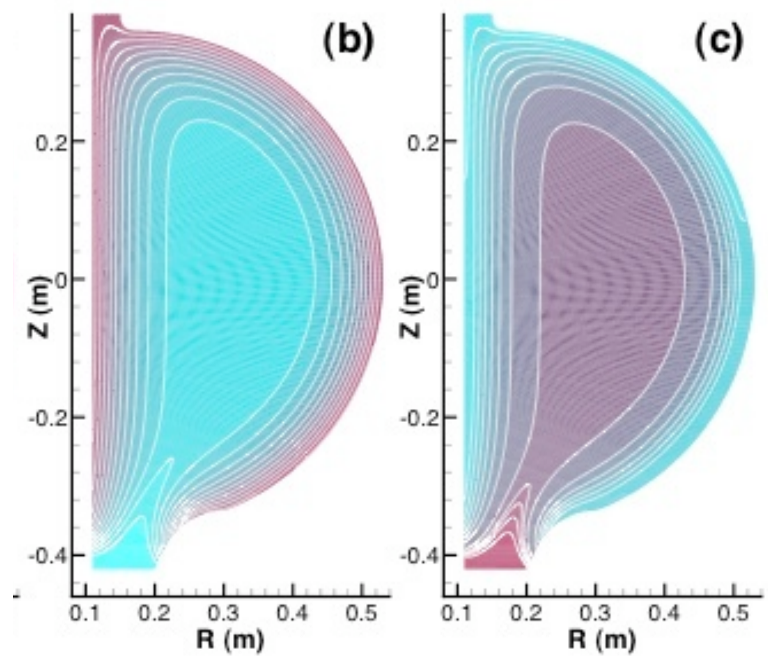


**The final distribution of the 6.5 mWb of poloidal flux is shown at left, and contours of $RB_\phi$ are shown at right.**

# More detailed modeling is applied to NSTX startup.

• The system of equations includes temperature and number-density evolution.

$$\frac{3}{2}n\left(\frac{\partial}{\partial t}+\mathbf{V}\cdot\nabla\right)T=-nT\,\nabla\cdot\mathbf{V}+\nabla\cdot\left[\left(\kappa_{||}-\kappa_{\perp}\right)\hat{\mathbf{b}}\hat{\mathbf{b}}+\kappa_{\perp}\mathbf{I}\right]\cdot\nabla T+\eta J^{2}$$

$$\frac{\partial n}{\partial t}+\nabla\cdot\left(n\mathbf{V}\right)=\nabla\cdot D\nabla n$$

• Transport coefficients are *T*-dependent: $\kappa_{||}$~$T^{5/2}$ ; $\eta$~$T^{-3/2}$ .

• Detailed modeling of the injector bank controls the injector voltage.

• The injector and absorber boundary conditions are swapped with respect to the HIT-II modeling.

- Tangential-**E** is applied at the injector.
- $\Delta I_{abs}$ is held at 0, presuming no absorber arc.
- The resulting flux-change starts from the injector for more accurate transient evolution.

# Boundary conditions for NSTX apply the circuit model and preclude drift of $I_{TF}$.

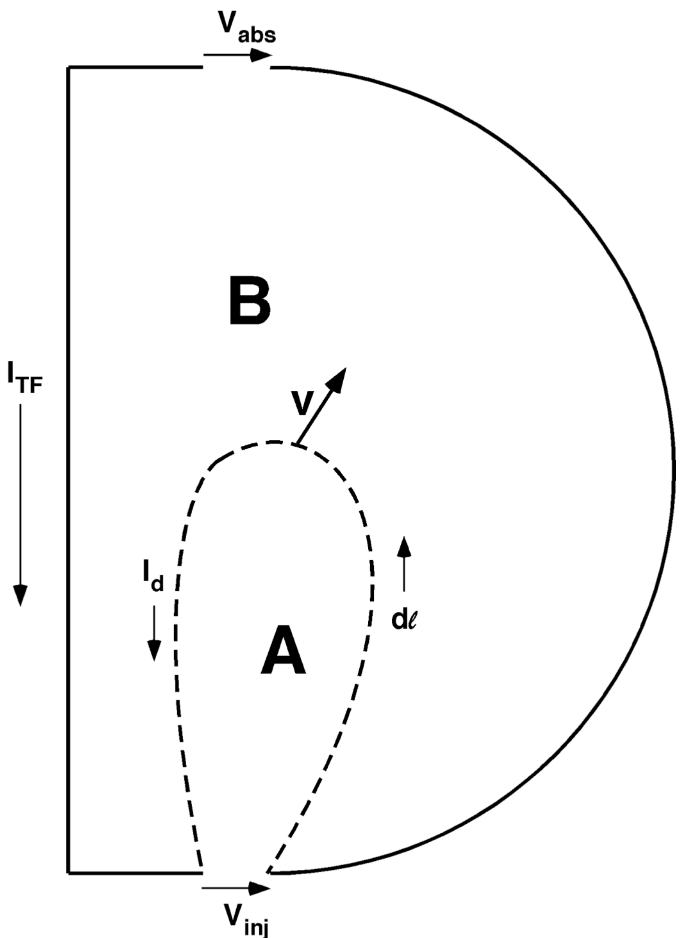


- Rate-of-change of toroidal flux — equals $V_{inj} - V_{abs}$
- Absorber-*I* — corresponds to a constant $I_{TF}$
- *T* near the absorber is kept low to maintain high resistivity in this region.
- Discharge (injector) current — measured by the change in $RB_\varphi$ just above the injector slot
- Toroidal flux — carried in by ExB flow at the injector and out by ExB flow at the absorber
- Equating flows of *vacuum* toroidal flux yields

$$E_r^{abs} = E_r^{inj} \frac{r_{inj,\min}}{r_{abs,\min}} \frac{\displaystyle\int_{r_{inj,\min}}^{r_{inj,\max}} dr \frac{B_\varphi}{r^2 B^2}}{\displaystyle\int_{r_{abs,\min}}^{r_{abs,\max}} dr \frac{B_\varphi}{r^2 B^2}}$$

Used to compute outward flow at absorber--not for a BC on **B**.



Fusion Energy Program

# The quantitative difference between the velocity boundary conditions used for HIT-II and NSTX is very small.

**The HIT-II calculations equated plasma flow**

- **The two conditions differ by a weighting factor 1/R in the integrals**
- **The resulting difference is $O(d_{slot}/R) << 1$**
- **Quantitative comparison of the plasma evolution found very small differences**

# The net toroidal-flux change in NSTX is << the flux injected at the bottom

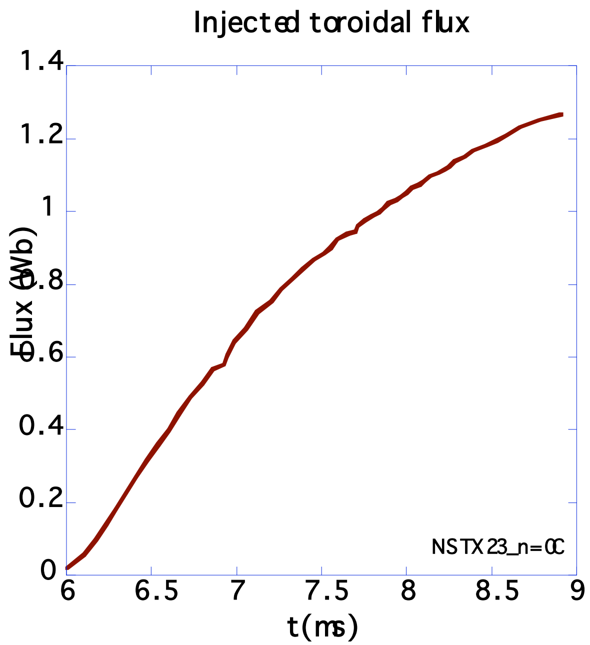


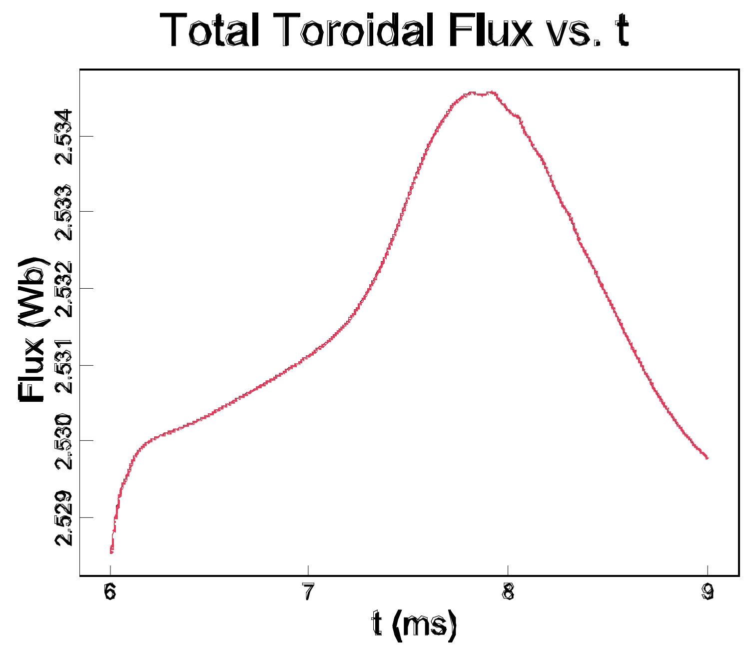


Total injected flux > 1 Wb

Net flux change < 0.005/2.5 = 0.2%



Fusion Energy Program

## **Pegasus injector modeling:** The small size and 3D geometry of the plasma guns requires a different approach.

• Current drive is modeled as a small source region within the domain and not through a boundary condition.

• Ohm's law accommodates the source, applied in the vicinity of the experiment's guns (first configuration in Pegasus):

$$\mathbf{E} + \mathbf{V} \times \mathbf{B} = \eta \mathbf{J} - \mathbf{E}_{inj}$$

• The applied source is parallel to the local magnetic field and has a Gaussian distribution in poloidal coordinates and in toroidal angle.

• Induced-**B** and **J** propagate Alfvénically along background-**B** (initially).

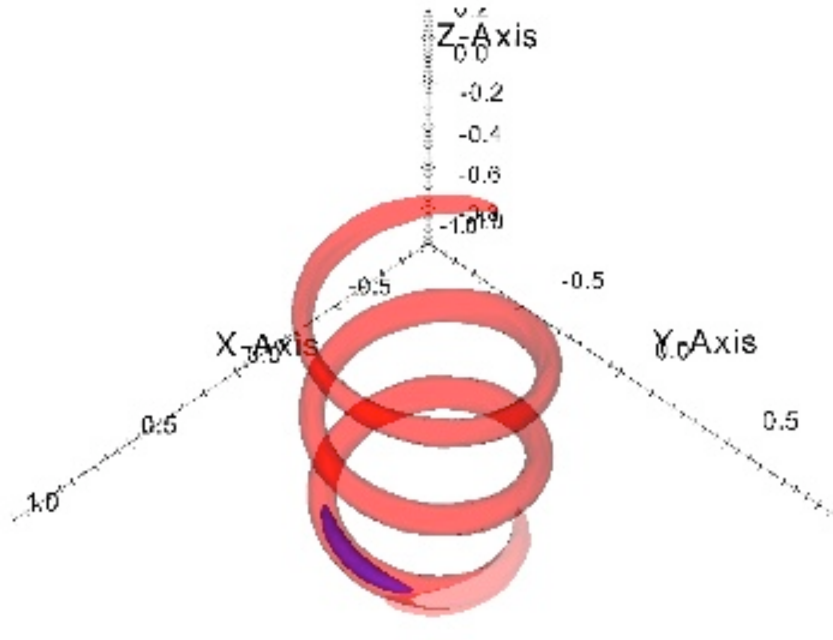


Effective applied $\mathbf{E}_{\parallel}$ (half-max shown in blue) and the resulting current channel ($\lambda \simeq 1\mathrm{m}^{-1}$ shown in red)

# Two non-standard boundary conditions are also used in the Pegasus modeling.

• Conductivity of the gun-heated channel with respect to background is critical, so temperature evolution and temperature-dependent resistivity are used.

• With Spitzer-$\eta$, fixed low-temperature boundary conditions preclude a conducting path to the walls.

• Insulating conditions with an auxiliary decay term, $-\alpha(T\text{-}T_{wall})$, allows the current to heat a path to the walls.

• An effective electrical wall decay rate is also used when advancing $B_\phi$ so that the net axial current of the channel does not compress toroidal flux.

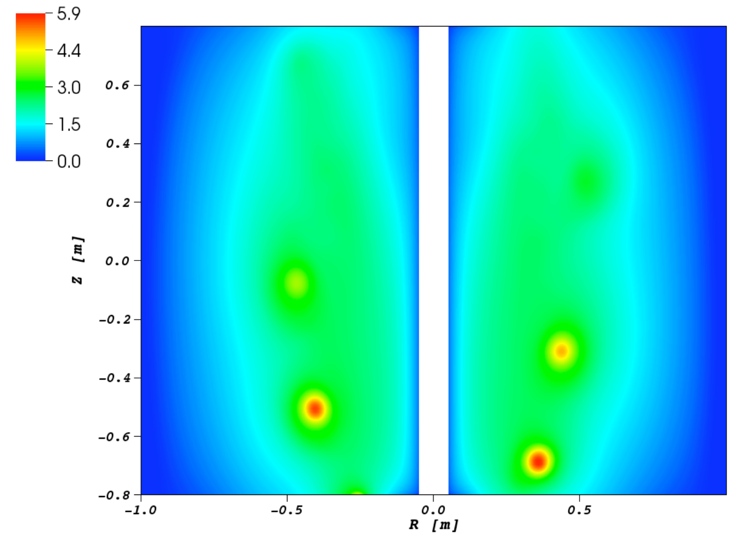


**Cross-section view of temperature early in time.**

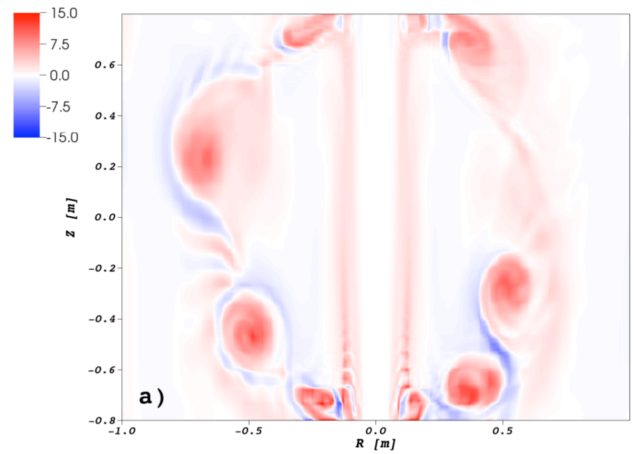


**Parallel current later when $I_p$=26kA.**